Neurobiology of Disease 124 (2019) 202–217

Contents lists available at ScienceDirect

Neurobiology of Disease

journal homepage: www.elsevier.com/locate/ynbdi

Naturally occurring autoantibodies against α-synuclein rescues memory and motor deficits and attenuates α-synuclein pathology in mouse model of Parkinson's disease

Ya-ru Huang[a,b,1], Xi-xiu Xie[a,1], Mei Ji[a,b], Xiao-lin Yu[a], Jie Zhu[a], Ling-xiao Zhang[a,b], Xiao-ge Liu[a,b], Chen Wei[c], Gang Li[d,*], Rui-tian Liu[a,*]

[a] National Key Laboratory of Biochemical Engineering, Institute of Process Engineering, Chinese Academy of Sciences, Haidian District, Beijing 100190, China
[b] School of Chemical Engineering, University of Chinese Academy of Sciences, Beijing 100049, China
[c] National Institutes for Food and Drug Control, Beijing 100050, China
[d] Department of Neurology, Union Hospital, Tongji Medical College, Huazhong University of Science and Technology, Jiefang Avenue, Wuhan 430022, China

ARTICLE INFO

Keywords:
Parkinson's disease
α-Synuclein
Naturally occurring autoantibodies
A53T mice
IVIG

ABSTRACT

It has been suggested that aggregation of α-synuclein (α-syn) into oligomers leads to neurodegeneration in Parkinson's disease (PD), but intravenous immunoglobulin (IVIG) which contains antibodies against α-syn monomers and oligomers fails to treat PD mouse model. The reason may be because IVIG contains much low level of antibodies against α-syn, and of which only a small part can penetrate the blood-brain barrier, resulting in an extremely low level of effective antibodies in the brain, and limiting the beneficial effect of IVIG on PD mice. Here, we first isolated naturally occurring autoantibodies against α-syn (NAbs-α-syn) from IVIG. Our further investigation results showed that NAbs-α-syn inhibited α-syn aggregation and attenuated α-syn-induced cytotoxicity in vitro. Compared with vehicles, NAbs-α-syn significantly attenuated the memory and motor deficits by reducing the levels of soluble α-syn, total human α-syn and α-syn oligomers, decreasing the intracellular p-α-syn^{ser129} deposits and axonal pathology, inhibiting the microgliosis and astrogliosis, as well as the production of proinflammatory cytokines, increasing the levels of PSD95, synaptophysin and TH in the brain of A53T transgenic mice. These findings suggest that NAbs-α-syn overcomes the deficiency of IVIG and exhibits a promising therapeutic potential for the treatment of PD.

1. Introduction

Dementia and movement disorders in the aging population, which includes Parkinson's disease (PD), dementia with Lewy bodies (DLB), and PD dementia (PDD), jointly known as Lewy body diseases (LBD), is common caused by neuronal accumulation of α-synuclein (α-syn) (Savica et al., 2013; McKeith and Burn, 2000; Trojanowski and Lee, 1998). It is estimated that over 10 million people in the world suffer from these diseases for which there is currently no cure (Savica et al., 2013). α-syn contains 140 amino acids (Jakes et al., 1994) and is predominantly expressed in neurons and concentrated at synaptic terminals (Murphy et al., 2000). Abnormal α-syn accumulation in synaptic terminals and axons may play an important role in the pathology of LBD (Roy et al., 2007; Bellucci et al., 2012; Games et al., 2013). α-syn monomers can aggregate into oligomers and fibrils, and it is widely accepted that α-syn oligomers rather than fibrils are the more neurotoxic species, which may damage synapses and dendrite (Gaugler et al., 2012; Scott et al., 2010). Moreover, α-syn oligomers can be released by neurons and lead to neurodegeneration and inflammation by propagating to other neurons and glial cells (Tsigelny et al., 2007; Lee et al., 2010; Desplats et al., 2009; Brundin et al., 2010). These effects of α-syn oligomers collectively contribute to the motor symptoms of PD, such as resting tremor, bradykinesia, rigidity of muscle tone and postural instability (Graham and Sidhu, 2010).

Strategies to remove existing oligomeric α-syn are believed to be essential to prevent PD progression. Preclinical studies suggested that active and passive immunization against α-syn may present probable strategies. However, given that active immunization of patients with Alzheimer's disease (AD) was accompanied with considerable side effects, such as meningoencephalitis (Robinson et al., 2004), passive

* Corresponding authors.
E-mail addresses: gangli2008@hust.edu.cn (G. Li), rtliu@ipe.ac.cn (R.-t. Liu).
[1] These authors equally contributed to this work.

https://doi.org/10.1016/j.nbd.2018.11.024
Received 5 August 2018; Received in revised form 20 November 2018; Accepted 23 November 2018
Available online 24 November 2018
0969-9961/

immunization is considered as a potentially safer alternative. Treatments with humanized or human monoclonal antibodies against α-syn have been investigated in pilot clinical trials. Passive immunization with antibody PRX002/RG7935 which bound to the C-terminus region of α-syn was tolerance in patients and reduced 97% free serum α-syn after a single infusion in phase I clinical trial (Jankovic et al., 2017). Another monoclonal antibody, BIIB054 (Biogen), which targets the N-terminus of α-syn, reduced spread of truncated α-syn species to contralateral cortex and rescued motor impairment in a mouse model exhibiting preformed fibrils, and was also tolerance in phase I clinical trial (Weihofen et al., 2016; Tarnow et al., 2016). Above two antibodies have both entered to phase II clinical trials, indicating that monoclonal antibody against α-syn is a therapeutic potential for PD treatment.

IVIG is an immune globulin product derived from the plasma of healthy young volunteers. Previous reports showed that IVIG contained NAbs-α-syn and could inhibit α-syn-induced neurotoxicity in vitro (Patrias et al., 2011; Smith et al., 2012). But it did not provide neuroprotective effect on the nigrostriatal system in the MPTP-treated PD mice (St-Amour et al., 2012). In the present study, we purified NAbs-α-syn from IVIG for the first time, investigated its properties and evaluated its therapeutic effect in vitro and in vivo.

2. Materials and methods

2.1. Materials

IVIG, which was manufactured from pooled plasma of a thousand healthy donors, was kindly provided by Shandong Taibang Biological Products Co., Ltd. (Taian, Shandong, China). The plasmid pT7-7 was kindly provided by Prof. Conggang Li (Wuhan Institute of Physics and Mathematics, Chinese Academy of Sciences, China).

2.2. Expression and purification of α-syn

α-syn was expressed and prepared according to the previous reports (Hoyer et al., 2002). α-syn oligomers were prepared as described by Pieri, L. et al (Pieri et al., 2016). Briefly, freshly prepared α-syn was diluted to 1 mg/mL with PBS, then incubated at 37 °C under constant stirring at 200 rpm. The aggregation states of α-syn was determined by Thioflavin T fluorescence assay. α-syn fibrils were prepared by incubating α-syn 7 days at 37 °C under constant stirring at 200 rpm. Then, the aggregated α-syn was centrifuged at 20, 000 × *g* for 30 min, and the precipitate was collected and resuspended in PBS.

2.3. Size exclusion chromatography (SEC)

500 μL aggregated α-syn oligomers were loaded onto Superose 6 10/300 GL column (GE Healthcare, Piscataway, USA) connected to an AKTA pure system (GE Healthcare). The column was pre-equilibrated and eluted with PBS at a flow rate of 0.5 mL/min. Eluting peaks which contained α-syn oligomers or monomers were collected for subsequent experiments.

2.4. Transmission electron microscopy (TEM)

10 μL α-syn monomers, oligomers or fibrils were applied to 200 mesh copper grids for 20 min, blotted with filter paper, and negatively stained with 2% uranyl acetate for 30 s, then blotted and air-dried. Samples were examined under a TEM (Hitachi H7650, Japan) with an operating voltage of 120 kV at 10, 000 × magnification.

2.5. NAbs-α-syn purification

NAbs-α-syn were isolated from IVIG using α-syn oligomers affinity chromatography as previously described with some modifications (Wang et al., 2016). The packing material coupled with α-syn oligomers for affinity chromatography was prepared by mixing 10 mg coupling UltraLink Biosupport resin (Thermo Scientific, Waltham, MA, USA) with 100 μL (1 mg/mL) α-syn oligomers in coupling buffer (0.2 M sodium carbonate, 0.6 M sodium citrate, pH 10) with shaking for 1 h at RT. The material was then washed and blocked with 500 μL of 3 M monoethanolamine (pH 9.0) with shaking for 2.5 h at 37 °C. For NAbs-α-syn isolation, IVIG was diluted 1:10 in 20 mM PBS (pH 7.4) and loaded onto the column. The column was washed with PBS, and the unbound antibodies, termed flow-through (Ft), were collected and used as a control. NAbs-α-syn was eluted with 0.2 M glycine in 2% acetic acid (pH 2.2) and immediately neutralized with 1 M Tris buffer (pH 9.0) to pH 4 to stabilize the antibody. Each batch of purified NAbs-α-syn was routinely tested by ELISA for binding capacity.

2.6. Dot blot

Dot blot was used to test the binding of purified α-syn antibodies to α-syn oligomers. Briefly, nitrocellulose membranes were marked with a pencil to guide sample application. Monomers, oligomers, and fibrils of α-syn (2 μg) were applied to the membranes, and the blots were blocked at RT with 5% nonfat milk in 20 mM PBS with 0.1% Tween 20 (0.1% PBST). The blots were then incubated with different primary antibodies including anti-α-syn antibody (Abcam, ab138501, 1:10000), NAbs-α-syn, IVIG, Ft, respectively, then washed thrice for 10 min each with 0.1% PBST, and incubated with relevant secondary antibodies in PBST for 1 h. Afterward, the blots were washed thrice and developed with an ECL chemiluminescence kit (Pierce Biotechnology, Rockford, IL, USA). The total human α-syn levels of soluble fraction and insoluble fraction in brain stems were detected by dot blot as described above using anti-α-syn antibody (Abcam, ab138501, 1:10000) as the primary antibody. Soluble oligomer level in the immunized mice were also determined by dot blot as described above using OC, a fibrillar oligomer antibody, as the primary antibody.

2.7. ELISA assay

To test the affinity of NAbs-α-syn, IVIG with α-syn oligomers, 1 μg α-syn oligomers were coated onto a 96-well plate at 4 °C overnight. The wells were blocked by 3% BSA in PBS. After washing with 0.1% PBST, then serial diluted NAbs-α-syn or IVIG were added to wells and incubated for an hour at 37 °C. Bound antibodies were detected by the goat-anti-human secondary antibody labeled with HRP and 3,3′,5,5′-tetramethylbenzidine (TMB). The absorbance was measured at 450 nm by a SpectraMax M5 microplate reader (Molecular Devices, LLC., Sunnyvale, CA, USA).

Level of MCP-1 in the brain stem homogenates were determined using the ELISA kit following the manufacturer's protocols (Biolegend, San Diego, CA). Briefly, soluble brain stem extracts were added to a 96-well ELISA plate and then reacted with relevant primary and secondary antibodies, and data were collected by Accuri C6 flow cytometer (Becton, Dickinson and Company, USA).

Soluble α-syn level in the immunized mouse brain stems were quantified via ELISA using α-syn immunoassay kits in accordance with the manufacturer's protocol (Thermo Scientific, Waltham, MA, USA). The soluble α-syn level were standardized to the brain tissue weight and expressed in picogram or nanogram of α-syn per gram of brain tissue.

2.8. Thioflavin T fluorescence assay

To determine whether purified NAbs-α-syn can inhibit α-syn aggregation, α-syn (71 μM) was incubated alone or with 0.5 μM NAbs-α-syn, IVIG and Ft, respectively. Samples were collected at 0, 12, 24, 36, 48, 60, 72, 84, 96, 108 h. The assay was performed by periodically adding 190 μL of 5 mM thioflavin T (ThT) in 50 mM phosphate buffer (pH 6.5) to 10 μL samples (10 μM). Fluorescence was measured in a 96-

well black plate by a Safire2™ microplate reader (Tecan Group Ltd., Männedorf, Switzerland) with excitation at 450 nm and emission at 482 nm. Each reading represented the average of three values determined by a time scan after subtracting the fluorescence contribution from the control solution. Each assay was performed in triplicate.

2.9. MTT assay

Quantification of cell viability via MTT assay was performed as previously described with some modifications (Kim et al., 2013). Briefly, N2a cells were maintained in a medium (DMEM/ High Glucose, HyClone Laboratories, Logan, UT, USA) containing 10% FBS, and 1% penicillin/streptomycin antibiotics, and in a 5% CO_2 atmosphere at 37 °C. Cells were harvested from flasks and plated in 96-well polystyrene plates with approximately 5000 cells/ 100 μL of medium per well. Plates were incubated at 37 °C for 12 h to allow the cells to attach. After 12 h, cells were treated with 1 μM α-syn oligomers in the absence or presence of 0.25 μM or 0.5 μM IVIG, Ft or NAbs-α-syn for 48 h. The same volume of 0.2 M glycine was added to the control cultures. Cell viability was determined by adding 25 μL of 5 mg/mL MTT to each well. After 3 h incubation at 37 °C, 150 μL DMSO was added. The absorbance at 570 nm and 630 nm was measured by a SpectraMax M5 microplate reader. Averages from six replicate wells were used for each sample and control, and each experiment was repeated thrice. Cell viability was calculated by dividing the absorbance of wells containing samples (corrected for background) by the absorbance of wells containing medium alone (corrected for background).

2.10. Passive immunotherapy

A53T transgenic mice, which overexpressed A53T mutant human α-syn under the mouse prion promoter and developed severe motor impairment and cognitive deficits by accumulation of α-syn at 9–16 months of age (Lee et al., 2002), were purchased from Beijing HFK Bioscience Co., Ltd. (Beijing, China), kept in the animal facility of Tsinghua University, and used for immunotherapy and behavioral tests. All experimental protocols were approved by the Institutional Animal Care and Use Committee. PD transgenic and WT mice (12 months of age) were given food and water ad libitum and kept in a colony room at 22 ± 2 °C temperature and 45% ± 10% humidity under a 12 h:12 h light/dark cycle. Groups of PD mice ($n = 6$) were administered subcutaneously with low (0.8 mg/kg mouse body weight), high (2.4 mg/kg mouse body weight) dose of NAbs-α-syn, IVIG, or Ft, for four weeks with one-week intervals. As controls, the WT and vehicle groups were treated with 0.2 M glycine (vehicle). The mice were trained and tested for their behavioral and cognitive abilities 5 d after the last administration, then sacrificed (10 d after the last treatment).

2.11. Body suspension test

Muscle strength of mice was tested by body suspension test as previously described (Metz and Schwab, 2004). The animals were suspended by their forelimbs to a metal bar with a diameter of 2 mm and the time was measured until the animals lost the bar and dropped down. Mice were tested three times.

2.12. Pole test

The pole test was utilized to measure motor coordination and balance in A53T mice. Mice were initially habituated and trained 1 d prior to testing. Then they were placed on the top of a rough-surfaced wooden pole (50 cm in length and 1 cm in diameter) and allowed to descend to the base of the pole. During the test, mice were placed with their heads oriented toward the top of the pole. The time required by the mice to turn their heads downward and to descend the entire length of the pole was measured. The best performance of each mouse over five consecutive trials was recorded.

2.13. Y-maze test

The spatial recognition memory of the mice was tested by the Y-maze test (Wang et al., 2017). Y-mazes were made of gray wood, covered with black paper, and consisted of three arms with an angle of 120 degrees between each arm. Each arm was 8 cm × 30 cm × 15 cm (width × length × height). The three identical arms were randomly designated as the start arm, in which the mouse started to explore (always open); the novel arm, which was blocked during the first trial but open during the second trial; and the other arm (always open). The Y-maze test consisted of two trials separated by an intertrial interval (ITI) to assess spatial recognition memory. The first trial (training) had a 10-min duration and allowed the mouse to explore only two arms (start arm and the other arm) of the maze, with the third arm (novel arm) being blocked. After a 1-h ITI, all three arms were accessible for the mice for the second trial. The mice were placed back to the starting arm, with free access to all three arms for 5 min, by using a ceiling-mounted charge-coupled device camera. All trials were recorded on a videocassette.

2.14. Brain lysate preparation and Western blot

Mice were deeply anesthetized with sodium pentobarbital, transcardially perfused with ice-cold PBS containing heparin (10 U/mL), and finally sacrificed. Their brains were immediately removed. The brainstems were removed from bregma −4.04 mm to −8.24 mm and divided along the sagittal plane. The brain tissues of A53T mice were homogenized in TNE buffer (10 mM Tris-HCl, pH 7.4, 150 mM NaCl, 5 mM EDTA) containing complete protease inhibitor mixture tablets (Millipore) and detergents (0.5% Nonidet P-40). The homogenate was centrifuged (5 min at 100, 000 ×g), and the supernatants were collected and termed as soluble fraction. The pellets were dissolved in 10% SDS, heated to 70 °C for 10 min, and then spun at 2, 000 ×g for 30 s. The new supernatants were considered to be the insoluble fraction. The protein concentrations of soluble and insoluble fractions were determined using the BCA protein assay (Thermo) according to the manufacturer's instructions.

For Western blot, proteins were separated by SDS-PAGE and transferred onto a nitrocellulose membrane (Millipore). After blocking for 2 h at room temperature with 5% nonfat milk, membrane was probed with anti-PSD95 antibody (Abcam, ab18258,1:1000), anti-synaptophysin antibody (Abcam, ab32127, 1:1000) and anti-TH antibody (Abcam, ab152, 1:1000), respectively, with β-actin as a loading control. Blots were washed thrice in 0.1% PBST, followed by incubating with the secondary antibodies for 1 h at room temperature. Then blots were washed thrice again and imaged in a Li-Cor Odyssey IR detection system (Odyssey). Densitometry was performed using the integrated intensity value for each band, and the results were expressed as the ratio of protein relative to β-actin.

2.15. Immunohistochemistry (IHC)

One brain hemisphere was fixed in 4% paraformaldehyde in PBS at 4 °C overnight and processed for paraffin-embedded sections. 5 μm sagittal paraffin-embedded sections were immunostained with anti-TH antibody (Abcam, ab152, 1:100), anti-phospho-Ser129-α-syn antibody (pSer129) (Abcam, ab59264, 1:100), anti-Iba-1 antibody (GeneTex, GTX100042, 1:100), and anti-GFAP antibody (Abcam, ab53554, 1:100), respectively, and followed by incubation with relevant HRP-labeled secondary antibody at 37 °C for 1 h, then visualized with diaminobenzidine (DAB).

All images were acquired with an Olympus IX73 inverted microscope with DP80 camera, and all analyses were performed blind to the genotype and treatment of the mice. We selected sections with similar

neuroanatomical regions of the brain stems and striatum for all histological analyses. At least three sections were analyzed per mouse, and three fields of view for each section were imaged. Immunofluorescence intensities and immunostaining areas were quantified using IpWin5 software.

2.16. Double immunolabeling

To determine the colocalization between α-syn and the neurofilament marker SMI312, double-labeling experiments were performed as described previously (Games et al., 2014). Paraffin sections were immunolabeled with the pSer129 antibody (Abcam, ab59264, 1:100) and the α-syn immunoreactive structures were detected with the goat-anti-rabbit secondary antibody (ZSGB-BIO, 1:100). SMI312 was detected with an FITC-tagged antibody (ZSGB-BIO, 1:100).

To determine the colocalization between α-syn and astrocyte or microglia, paraffin sections were immunolabeled with pSer129 or LB509 antibody and anti-GFAP or anti-Iba-1 antibody, respectively, α-syn was detected with the goat-anti-rabbit or goat-anti-mouse secondary antibody (ZSGB-BIO, 1:100), respectively. GFAP was detected with an FITC-tagged goat-anti-mouse antibody (ZSGB-BIO, 1:100). Iba-1 was detected with an FITC-tagged goat-anti-rabbit antibody (ZSGB-BIO, 1:100). All sections were processed simultaneously under the same conditions and experiments were performed in triplicate to assess the reproducibility of results. The images were obtained with a confocal microscopy (Leica TCS SP5, 63× objective).

2.17. Uptake of α-syn oligomers in cells

BV-2 cells were plated at a density of 1×10^5 cells into in a 12 well plate on the day before the experiment. 1 μM α-syn oligomers were pre-incubated with either 0.25 μM NAbs-α-syn, IVIG, Ft or 0.2 M glycine (Con) for 10 min at room temperature to form NAbs-α-syn-α-syn immune complex. Then these mixtures were added to cells with culture media. Cells were then incubated at 37 °C for 24 h. Immunofluorescence staining of BV2 cells for α-syn and Fcγ receptor was conducted as previously described (Lee and Lee, 2002). Briefly, cells were fixed in 4% paraformaldehyde for 20 min after washing with PBS three times (5 min each wash), and permeabilized in 0.3% Triton X-100. Then cells were incubated in blocking solution (10% goat serum in PBS), and followed by incubation with LB509 antibody and CD16/CD32 monoclonal antibody (BD, 553142, 1:100). The α-syn immunoreactive structures were detected with the goat-anti-mouse secondary antibody (ZSGB-BIO, 1:100). Fcγ receptor was detected with an FITC-tagged goat-anti-rat antibody (ZSGB-BIO, 1:100).

2.18. Statistical analysis

All quantitative analyses were performed under blinded conditions. Statistical significance was tested using one-way ANOVA analysis by LSD (SPSS 16.0 software) or Tukey's test (GraphPad Prism 6.0). Results were expressed as group mean ± SEM, and $P < .05$ was considered statistically significant.

3. Results

3.1. Binding of NAbs-α-syn to α-syn oligomers

For the present study, we expressed and purified α-syn, and produced oligomers and fibrils from recombinant human α-syn. Oligomers were further purified by SEC. Monomers presented in the fraction 23 mL, while oligomers presented in the fractions 17–22 mL, indicating these oligomers may be low molecular weight oligomers (Fig. 1A). Oligomers and monomers were collected and then confirmed by TEM. The results showed that α-syn oligomers appeared as a heterogeneous mixture of curvy, globular, and short elongated structures, and α-syn monomers appeared as black spots, while α-syn fibrils were in amorphous reticular structure (Fig. 1B). Then we prepared affinity chromatography resin coupled with α-syn oligomers, which was used for the isolation of NAbs-α-syn. The affinity of obtained NAbs-α-syn to α-syn monomers, oligomers, and fibrils were detected by dot blots using 0.5 μg/mL of NAbs-α-syn, IVIG, Ft and anti-α-syn monoclonal antibody, respectively. The results showed that anti-α-syn antibody recognized the monomers, oligomers, and fibrils of α-syn (Fig. 1C), which was consistent with previous report (Plotegher et al., 2017). NAbs-α-syn showed more binding to α-syn oligomers, less binding to α-syn monomers, and no binding to fibrils, while IVIG and Ft did not show obvious binding to any α-syn morphologies (Fig. 1C). When the concentration of IVIG and Ft increased to 5 μg/mL, IVIG showed the binding to the monomers, oligomers, and fibrils of α-syn (Fig. 1D), while Ft showed less binding to the monomers and fibrils in contrast to IVIG, and almost no binding to the oligomers (Fig. 1D, E), which further suggested that NAbs-α-syn contained concentrated antibodies mainly against α-syn oligomers and monomers, and IVIG contains many different monoclonal antibodies recognizing monomers and different α-syn aggregated states. Moreover, our ELISA results showed that NAbs-α-syn exhibited much higher affinity to oligomers than IVIG by 75 times (Fig. 1F), further indicating that the antibodies against α-syn oligomers had much higher concentration in NAbs-α-syn, which was concentrated from IVIG.

3.2. NAbs-α-syn inhibits α-syn aggregation

ThT fluorescence assay was performed to determine the effect of NAbs-α-syn on α-syn aggregation. When incubated alone, α-syn showed the expected time-dependent increase in fluorescence. When α-syn was co-incubated with NAbs-α-syn, α-syn aggregation was completely inhibited (Fig. 1G). By contrast, IVIG slightly inhibit α-syn aggregation and almost no inhibition of α-syn aggregation was observed when α-syn was co-incubated with Ft.

3.3. NAbs-α-syn attenuates α-syn cytotoxicity

MTT assay is widely used to determine cell viability and cellular response to α-syn. N2a cells were treated with aggregated α-syn in the absence or presence of Ft, IVIG, or NAbs-α-syn to determine the effects of NAbs-α-syn on α-syn-mediated cellular toxicity. The results showed that 1 μM α-syn oligomers remarkably reduced cell viability, Ft had no significant influence on the α-syn-mediated cellular toxicity, while high dose (0.5 μM) IVIG attenuated α-syn cytotoxicity, NAbs-α-syn significantly improved cell viability relative to IVIG in a dose-dependent manner (Fig. 1H).

3.4. NAbs-α-syn attenuates motor performance and memory deficits in A53T mice

Impaired balance and coordination is a primary symptom of PD patients (Meredith and Kang, 2006). Pole test and body suspension test were performed to assess the effects of NAbs-α-syn treatment on the balance and coordination of transgenic A53T mice. The results showed that vehicle- and Ft-treated A53T mice took a longer time to descend (Fig. 2A) and turn (Fig. 2B) from the pole compared with the WT littermates. NAbs-α-syn-H, NAbs-α-syn-L and IVIG rather than Ft significantly reduced movement initiation and descending time.

Muscle coordination and grip strength of fore- and hind-limbs were assessed by suspending the mice to a bar. The results revealed that WT mice were able to grasp the bar with the forelimbs for almost 50 s, but the hold time of vehicle-treated A53T mice was reduced to 17 s. Treatment with NAbs-α-syn-H, but not NAbs-α-syn-L, IVIG and Ft significantly increased the hold time (Fig. 2C). Moreover, NAbs-α-syn increased the hold time of A53T mice in a dose-dependent manner (Fig. 2C).

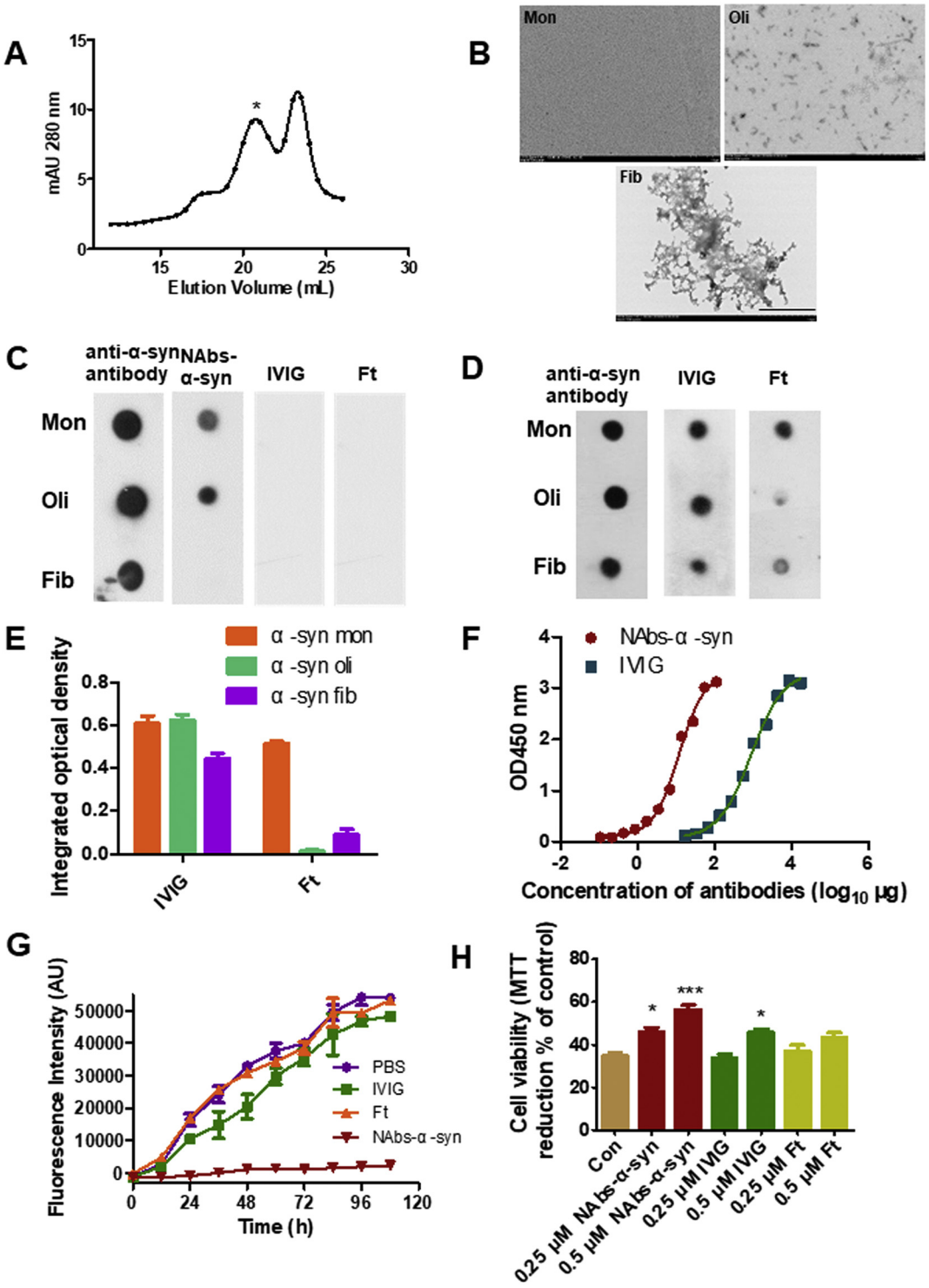

Fig. 1. The binding of NAbs-α-syn to α-syn and the effect of NAbs-α-syn on α-syn aggregation and α-syn-induced cytotoxicity. (A) Size exclusion chromatography of α-oligomers. 500 μL aggregated α-syn were loaded onto Superose 6 10/300 GL column which was pre-equilibrated and eluted with PBS. Oligomers (asterisk) and monomers presented in the 20 mL and 23 mL fractions, respectively. (B) TEM images of α-syn monomers, oligomers and fibrils. The sample were applied to copper grids, negatively stained and imaged by Hitachi TEM at 120 KV at 10, 000× magnification. Scale bars: 1 μm. (C, D) The binding of NAbs-α-syn to α-syn. Monomers, oligomers and fibrils were spotted onto nitrocellulose membrane (2 μg per dot) and probed with 0.5 μg/mL (C) or 5 μg/mL (D) of anti-α-syn antibody, NAbs-α-syn, IVIG and Ft, and appropriate second antibodies, respectively. The data from (D) were quantified using IpWin5 software (E). (F) The binding of NAbs-α-syn or IVIG to α-syn oligomers. NAbs-α-syn or IVIG were 2-fold serially diluted and tested in duplicates by ELISA against α-syn oligomers. (G) The effect of NAbs-α-syn on α-syn aggregation. α-syn (71 μM) was incubated with or without IVIG, NAbs-α-syn and Ft at 37 °C. Thioflavin T fluorescence was measured at different incubation time by mixing ThT solution with samples. (H) The effect of NAbs-α-syn on the α-syn cytotoxicity. N2a cells were incubated with α-syn oligomers (1 μM) in the absence or presence of 0.25 μM or 0.5 μM Ft, IVIG or NAbs-α-syn, respectively. α-syn incubated with the same volume of antibody buffer (0.2 M glycine, pH = 4) was used as a control (Con). The viability of the cells was analyzed by the MTT assay. Statistical analysis: one-way ANOVA followed by LSD (compared with α-syn alone, *$p < .05$, ***, $P < .001$).

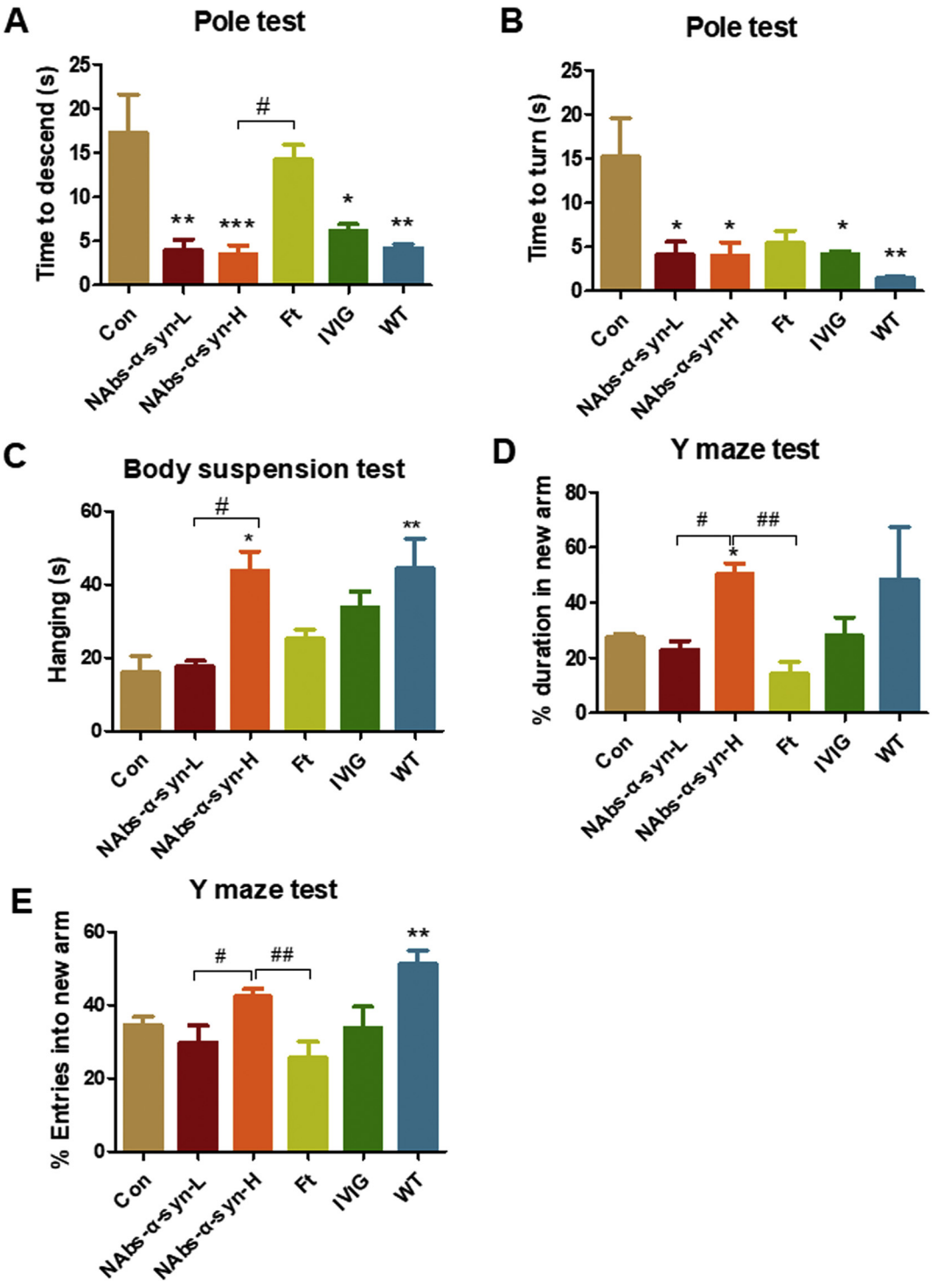

Fig. 2. NAbs-α-syn attenuated motor and memory deficits in A53T α-syn mice. A53T transgenic mice were treated with glycine (Con), low dose (L, 0.8 mg/kg) or high dose (H, 2.4 mg/kg) of NAbs-α-syn, Ft or IVIG (2.4 mg/kg), respectively, and their motor performance and memory were detected via pole test (A, B), body suspension test (C), Y maze (D, E), respectively. (A, B) The time of mice took to descend from the pole (A) and turn their hands on the pole (B) were recorded and analyzed by one-way ANOVA followed by Tukey's test. (C) Body suspension test was used to detect mouse muscle by recording the time in which the mice hold on the rung. Statistical analysis: one-way ANOVA followed by Tukey's test. (D, E) The recognition was detected via the time of mice spent in the new arm during the 5 min-trail (D) and times that mice entered into new arm (E). Statistical analysis: one-way ANOVA followed by LSD (compared with Con, *$p < .05$, **$p < .01$, ***, $P < .001$, compared with NAbs-α-*syn*-H, $^{\#}p < .05$, $^{\#\#}p < .01$).

Y-maze tests were conducted to evaluate the effect of NAbs-α-syn on cognitive function in A53T mice. The results showed that high dose of NAbs-α-syn-treated mice spent more time in the new arm (Fig. 2D) and exhibited more times in entering into the new arm than the vehicle-treated mice (Fig. 2E). No significant difference was observed between the control and Ft-, IVIG-, or NAbs-α-syn-L-treated groups. Taken together, these results indicated that NAbs-α-syn attenuated motor performance and cognitive impairment in PD transgenic mice.

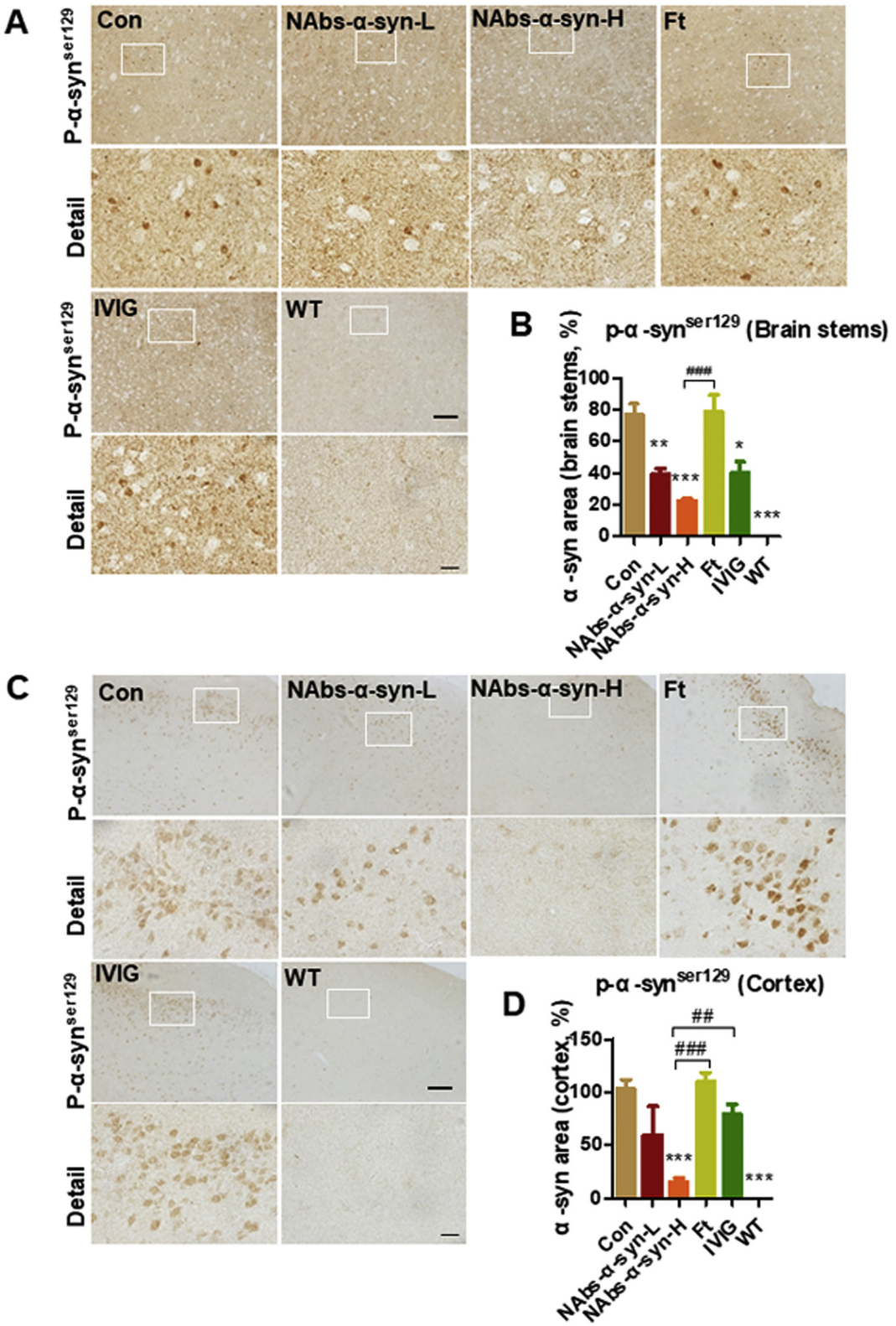

Fig. 3. NAbs-α-syn reduced α-syn level in A53T mouse brains. (A, C) Representative low and high photomicrographs of p-α-syn^{ser129} immunoreactivity in brain stems (A) and cortex (C) of WT mice and A53T mice treated with or without NAbs-α-syn, Ft or IVIG were detected by IHC using phospho-Ser129-α-synuclein antibody. (B, D) α-syn levels in the brain stems (B) and cortex (D) were quantified using IpWin5 software. Statistical analysis: one-way ANOVA followed by Tukey's test. (Low magnification scale bar = 100 μm and high magnification scale bar = 20 μm, compared with Con, *$p < .05$, **$p < .01$, ***, $P < .001$, compared with NAbs-α-syn-H, $^{\#\#}p < .01$, $^{\#\#\#}p < .001$).

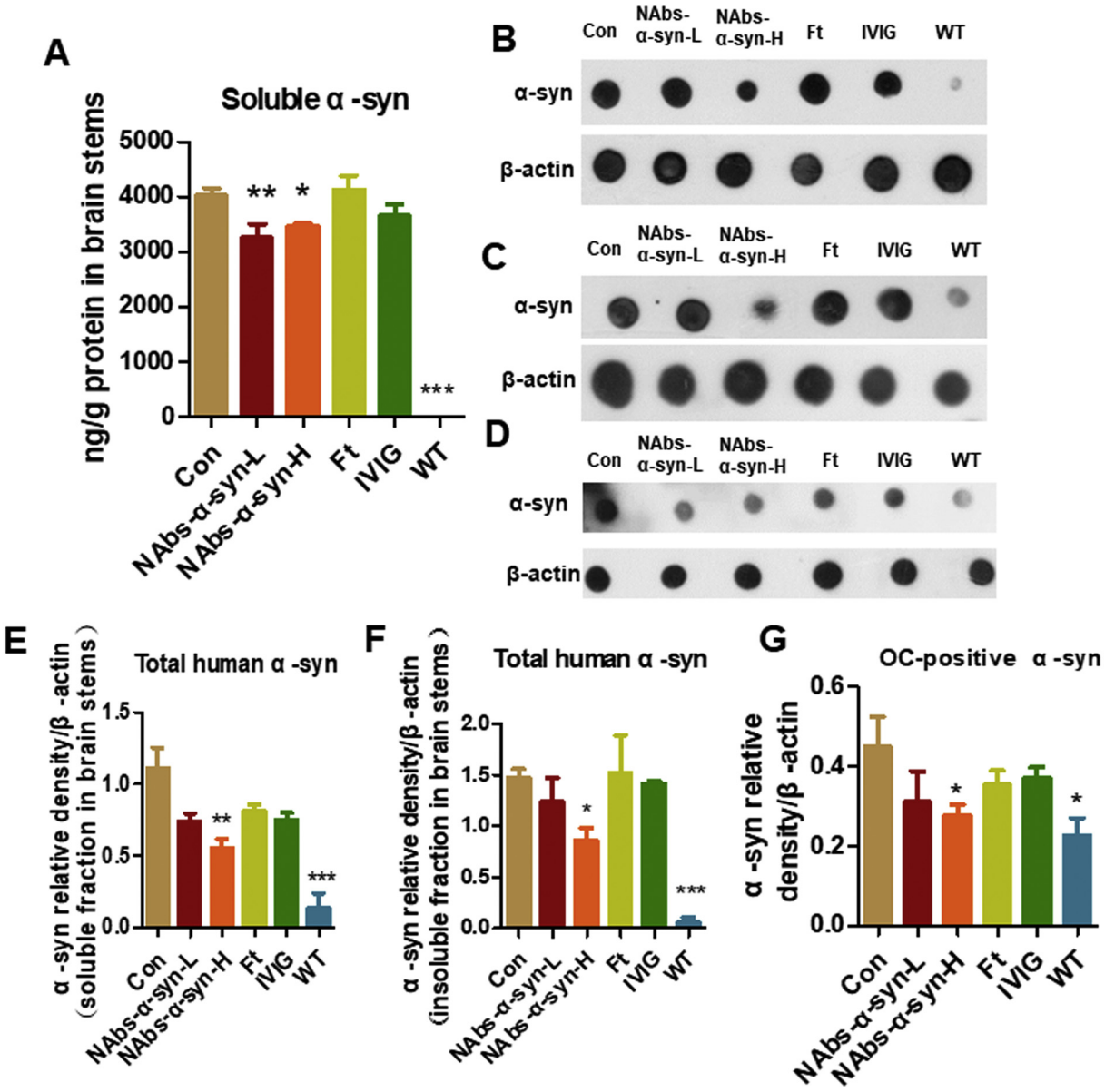

Fig. 4. NAbs-α-syn reduced α-syn level in A53T mouse brains. (A) Soluble α-syn abstracted from PD mouse control, NAbs-α-syn-, Ft- or IVIG-treated mice and WT was measured by ELISA, and the data was analyzed by one-way ANOVA followed by LSD. (B, C) The levels of total human α-syn in soluble fraction (B) or insoluble fraction (C) of brain stems of WT mice and A53T mice treated with or without NAbs-α-syn, Ft or IVIG were measured by dot blot with anti-α-syn antibody, and then the data were quantified using IpWin5 software (E, F). (D) The level of α-syn oligomers in brain stems of WT mice and A53T mice treated with or without NAbs-α-syn, Ft or IVIG were measured by dot blot with OC antibody, and then the data were quantified using IpWin5 software (G). Statistical analysis: one-way ANOVA followed by LSD (compared with Con, *p < .05, **p < .01, ***, P < .001).

3.5. NAbs-α-syn reduces α-syn level in A53T α-syn mouse brains

The levels of α-syn and α-syn oligomers in the brains of A53T mice are correlated with disease onset (Lee et al., 2002). To determine the effect of passive immunotherapy with NAbs-α-syn on phospho-Ser129 α-synuclein (p-α-syn^{ser129}) level, p-α-syn^{ser129} in brain stems and cortex were detected by IHC using pSer129 antibody. The control PD mice exhibited robust p-α-syn^{ser129} immunoreactivity in the brain stems (Fig. 3A, B) and cortex (Fig. 3C, D), whereas NAbs-α-syn-H, NAbs-α-syn-L and IVIG significantly decreased p-α-syn^{ser129} level in the brain stems and only NAbs-α-syn-H significantly reduced p-α-syn^{ser129} level in the cortex. Consistently, Ft treatment did not decrease the levels of p-α-syn^{ser129} in the brain stems and cortex of A53T mice.

Soluble α-syn level were further measured in the brain homogenates of PD mice by ELISA. The results showed that NAbs-α-syn-H and NAbs-α-syn-L significantly decreased the level of soluble α-syn in the PD mouse brainstems compared with the vehicle (Fig. 4A), IVIG-treated and Ft-treated groups did not show apparent changes in soluble α-syn level.

To investigate the effect of NAbs-α-syn treatment on the total human α-syn level, we applied dot blot using anti-α-syn antibody. As shown in Fig. 4B, C, E, F, NAbs-α-syn-H rather than Ft, IVIG, or NAbs-α-syn-L significantly reduced total human α-syn levels in soluble and insoluble fractions of brain stems.

To investigate the effect of NAbs-α-syn treatment on the α-syn oligomer level, we applied dot blot using OC antibody, mainly recognizing α-syn fibrillar oligomers (Kayed et al., 2007; Liu et al., 2015). As shown in Fig. 4D, G, NAbs-α-syn-H rather than Ft, IVIG, or NAbs-α-syn-L significantly reduced OC-positive α-syn oligomers.

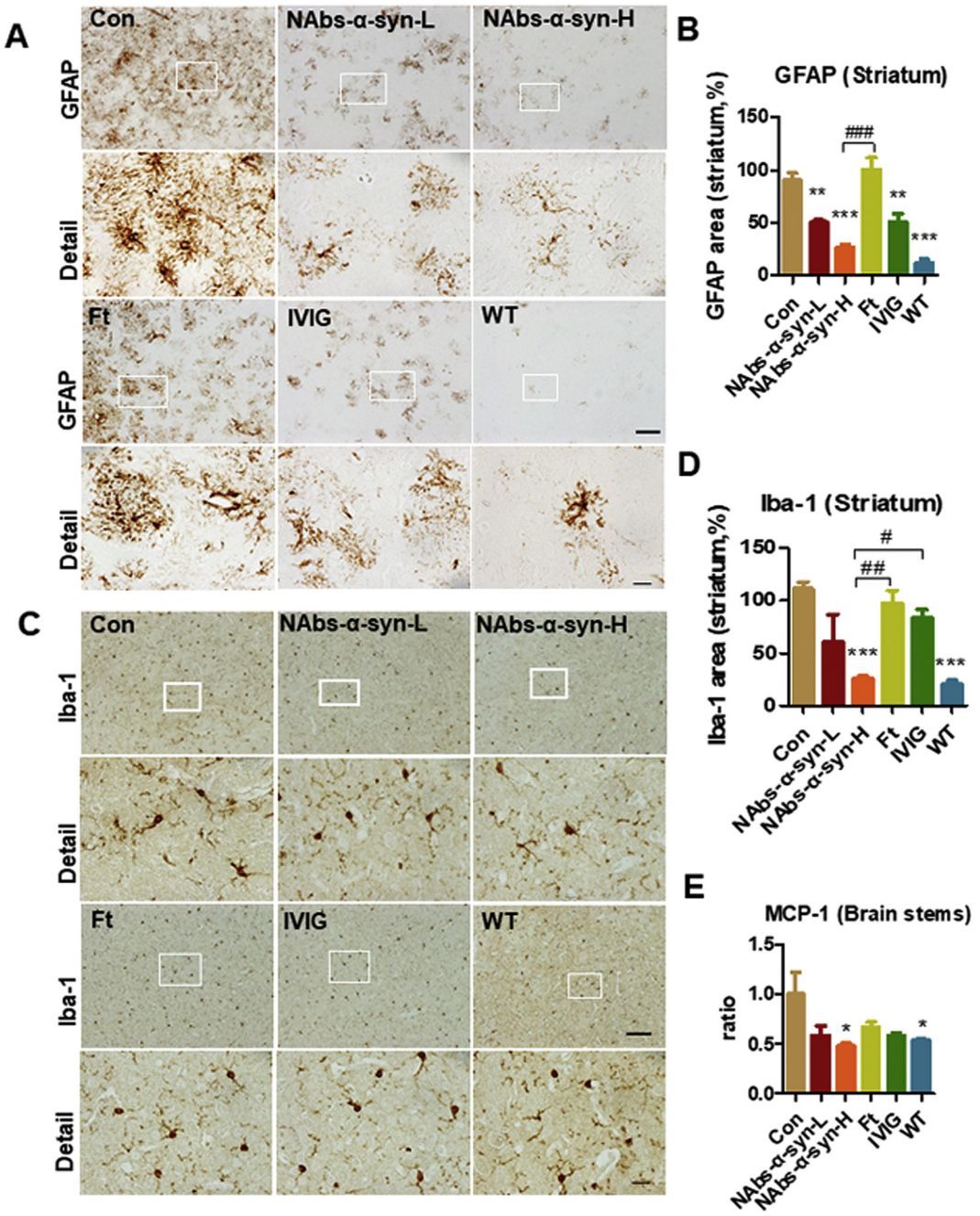

Fig. 5. NAbs-α-syn reduced neuroinflammation in A53T α-syn mouse brains. (A) Astrogliosis in the striatum were determined by IHC using glial fibrillary acidic protein (GFAP) monoclonal antibody, and then the stained astrocytes were quantified using IpWin5 software (B). (C) Microgliosis in the striatum of brain slices were detected by IHC using ionized calcium-binding adaptor molecule-1 (Iba-1) polyclonal antibody, and then the stained microglia were quantified using IpWin5 software (D). (E) NAbs-α-syn decreased the level of MCP-1 in A53T mouse brains. TNE-soluble α-syn fractions in brain stems of WT mice and A53T mice treated with or without NAbs-α-syn, Ft or IVIG were used to detect the level of MCP-1 using ELISA kits. Results were expressed as the ratio of OD value relative to A53T mouse control. Scale bar, 100 μm. Statistical analysis: one-way ANOVA followed by Tukey's test (Low magnification scale bar = 100 μm and high magnification scale bar = 20 μm, compared with Con, $^{*}p < .05$, $^{**}p < .01$, $^{***}p < .001$, compared with NAbs-α-*syn*-H, $^{\#}p < .05$, $^{\#\#}p < .01$, $^{\#\#\#}p < .001$).

3.6. NAbs-α-syn attenuates gliosis and decreases the level of inflammation factors in the brains of A53T mice

The activated astrocytes and microglia is linked to the pathogenesis of A53T mice (Ouchi et al., 2009). To detect the effect of NAbs-α-syn on astrogliosis and microgliosis in the brains of A53T mice, we stained astrocytes and microglia with antibodies against GFAP and Iba-1, respectively. PD transgenic mice showed remarkable astrocytosis and microgliosis in the striatum compared with WT mice. NAbs-α-syn-H, NAbs-α-syn-L, IVIG rather than Ft significantly reduced astrocytosis (Fig. 5A, B), but only NAbs-α-syn-H significantly decreased microgliosis (Fig. 5C, D).

Cytokines secreted by activated microglia and astrocytes also play an important role in the PD processes. The level of pro-inflammation factor MCP-1 in PD mice treated with antibodies were detected by ELISA kits. Consistent with the results of activated microglia in the mouse brains, NAbs-α-syn-H, but not Ft, NAbs-α-syn-L and IVIG significantly reduced the level of MCP-1 in the mouse brain stems (Fig. 5E). These results indicated that NAbs-α-syn effectively attenuated the inflammation in PD mouse brains.

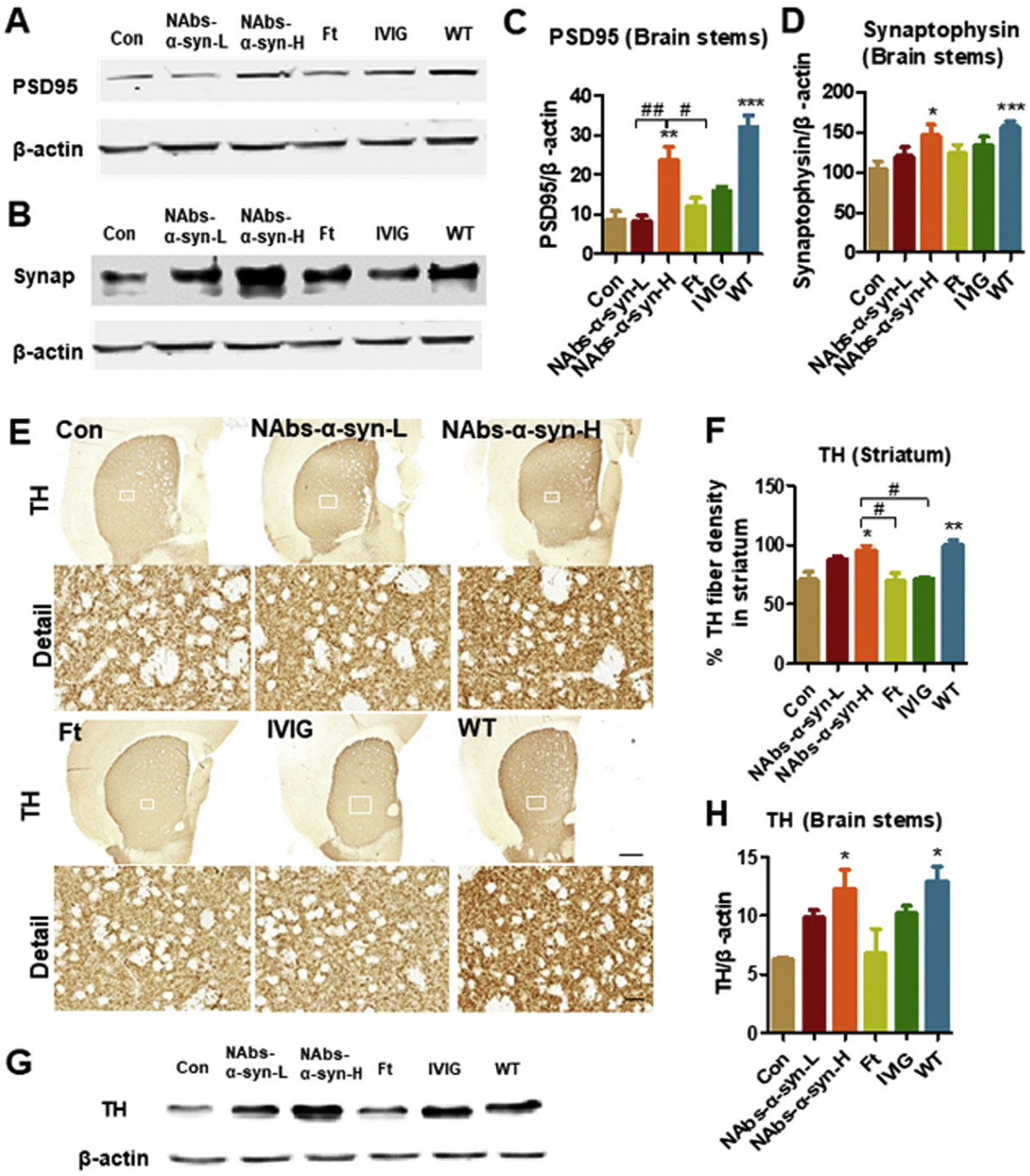

Fig. 6. NAbs-α-syn attenuated synaptic damage and increased TH level in A53T mouse brains. (A, B) Postsynaptic marker PSD95 (A) and presynaptic marker synaptophysin (B) in the brain stems were detected by Western blot. (C, D) The levels of PSD95 (C) and synaptophysin (D) were quantified using image studio software. (E) Representative striatal sections stained for TH immunoreactivity. (F) Quantification of TH fiber densities in the striatum using IpWin5 software. (G) TH level in the brain stems were detected by Western blot and then quantified by image studio software (H). Statistical analysis: one-way ANOVA followed by Tukey's test (Low magnification scale bar = 500 μm and high magnification scale bar = 20 μm, compared with Con, *p < .05, **p < .01, ***p < .001, compared with NAbs-α-syn-H, $^{\#}p < .05$, $^{\#\#}p < .01$).

3.7. NAbs-α-syn attenuates neuropathology in A53T mice

We further explore the effects of NAbs-α-syn on synaptic and TH pathology in A53T mice by Western blot and IHC analysis. PSD-95, one of the most abundant proteins in the postsynaptic density of excitatory synaptic, plays an important role in regulating synaptic transmission and plasticity (Hunt et al., 1996; Migaud et al., 1998). As shown in Fig. 6A, C, PSD95 level in the soluble brain stem homogenates of PD mice significantly increased with the treatment of NAbs-α-syn-H. However, no apparent difference in PSD95 level was detected between the control and the other PD mouse groups. NAbs-α-syn also attenuated synaptic pathology of PD mouse brain stems in a dose-dependent way. In order to further confirm the effect of NAbs-α-syn on synaptic pathology, synaptophysin (a presynaptic marker) was detected via Western blot using anti-synaptophysin antibody. The results showed that NAbs-α-syn-H rather than Ft, IVIG, or NAbs-α-syn-L significantly increased synaptophysin level (Fig. 6B, D).

TH is the limiting enzyme in DA synthesis (Arawaka et al., 2014).

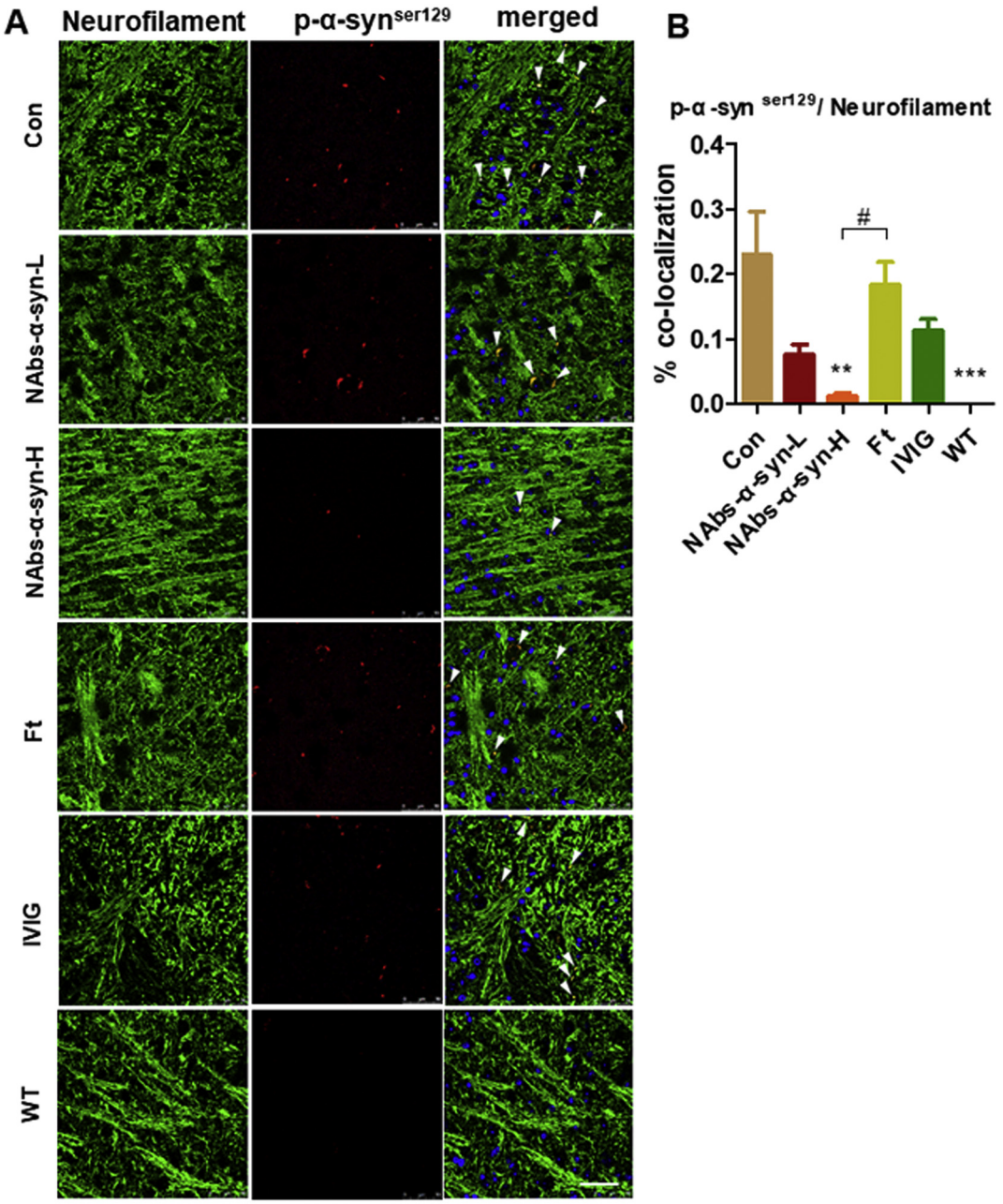

Fig. 7. NAbs-α-syn reduced intracellular p-α-syn^{ser129} level in neurons. (A) A53T tg mice were treated with vehicle, low dose or high dose of NAbs-α-syn, Ft or IVIG, respectively. The neuropil and α-syn deposits in the brain stems were detected by anti-neurofilament marker (SMI312) and anti-α-syn antibody pSer129, respectively and then the data were quantified using IpWin5 software (B). Statistical analysis: one-way ANOVA followed by Tukey's test (compared with Con, **P < .01, ***p < .001, compared with NAbs-α-syn-H, $^{\#}$p < .05).

The level of TH were quantified to evaluate the effect of NAbs-α-syn on the dopaminergic (DA) signaling pathway. The IHC results showed that TH-fiber densities in striatum were significantly increased by the treatment of NAbs-α-syn-H, but not NAbs-α-syn-L, IVIG, and Ft (Fig. 6E, F). Consistently, Western blot analysis also showed that TH level were significantly decreased in the brain stems of A53T mice compared with those of the WT littermates, whereas NAbs-α-syn-H, but not IVIG, NAbs-α-syn-L or Ft, significantly increased TH level (Fig. 6G, H).

3.8. NAbs-α-syn ameliorates the level of α-syn in neurofilaments in A53T mice

Previous studies have found that α-syn aggregates obviously accumulated in axons in PD patients and transgenic mice, followed by transferring between neurons and then damaged to the other neurons (Overk and Masliah, 2014). To determine whether passive immunization reduced accumulation of p-α-syn^{ser129} in the axons, double-labeling studies were performed with a monoclonal antibody against neurofilaments (SMI312) and the pSer129 antibody. There was obvious that p-α-syn^{ser129} accumulation in the axons of A53T mouse brain stems (Fig. 7A). NAbs-α-syn significantly reduced these p-α-syn^{ser129} deposits in a dose-dependent way, whereas IVIG and Ft did not show significant effect on it (Fig. 7B).

3.9. NAbs-α-syn reduces the level of p-α-syn^{ser129} in astrocyte in A53T mice

Previous reports showed that p-α-syn^{ser129} deposits appear frequently in astrocytes (Rostami et al., 2017; Gustafsson et al., 2017). We

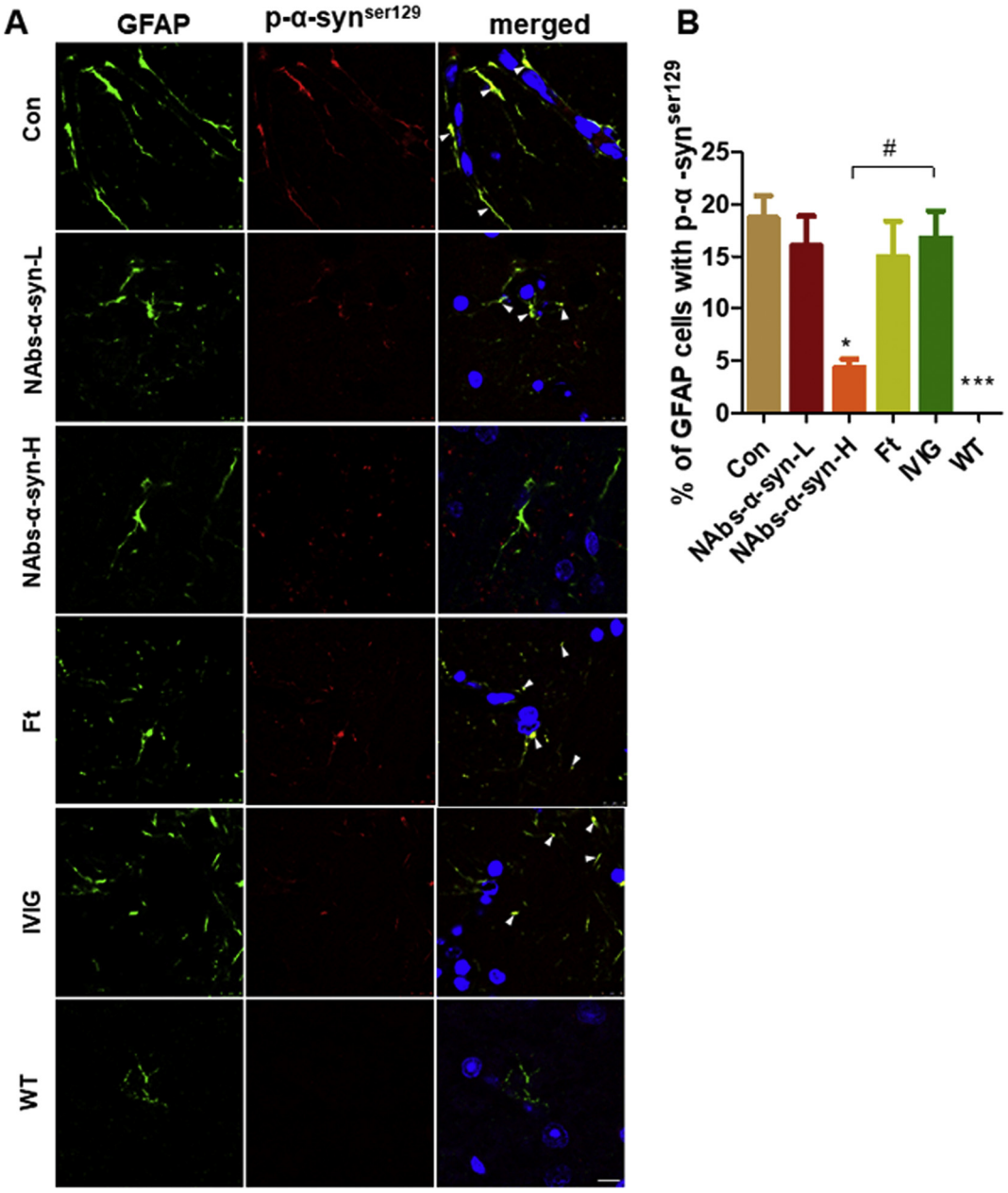

Fig. 8. NAbs-α-syn reduced the level of p-α-syn^{ser129} in astrocytes. (A) A53T tg mice were treated with vehicle, low dose or high dose of NAbs-α-syn, Ft or IVIG, respectively. The astrocyte and p-α-syn^{ser129} deposits in the brain stems were detected by anti-GFAP and anti-α-syn antibodies, respectively, then the data were quantified using IpWin5 software (B). Arrowheads indicate colocalization of p-α-syn^{ser129} and astrocytes. Scale bar, 10 μm. Statistical analysis: one-way ANOVA followed by Tukey's test (compared with Con, $^{*}P < .05$, $^{***}p < .001$, compared with NAbs-α-syn-H, $^{\#}p < .05$).

used double immunolabeling to detect the p-α-syn^{ser129} deposits in astrocytes. The results showed that compared with control, the mice treated with the NAbs-α-syn-H, but not NAbs-α-syn-L, Ft, IVIG exhibited lower p-α-syn^{ser129} deposits in GFAP-positive astroglial cells (Fig. 8A, B).

3.10. NAbs-α-syn promotes clearance of α-syn by microglia in A53T mice

As microglial cells can phagocytose α-syn and clear out extracellular α-syn aggregates, we detected α-syn in microglia using double immunofluorescence staining. The results showed that NAbs-α-syn rather than IVIG and Ft significantly increased the α-syn level in the microglia in the brain stems of the PD mice in a dose-dependent way (Fig. 9 A, B). These results suggested that NAbs-α-syn promoted uptake of α-syn by microglia cells.

3.11. NAbs-α-syn complex increases the level of Fcγ receptors on microglia

Fcγ receptors on macrophage and microglia recognize the Fc domains of IgG and trigger a wide variety of immune effector functions, including phagocytosis, antibody-dependent cellular cytotoxicity, and immune complex clearance (Gessner et al., 1998). In order to investigate whether antibody-α-syn complex was taken by neurons or microglia, we added the complex to the neuron or microglia cells, then α-syn and Fcγ receptor were detected. The results showed that the complex was mainly engulfed by microglia (Fig. 10A) rather than neurons (data not shown), which was consistent with previous reports (Bae et al., 2012). Quantitative analysis showed that NAbs-α-syn-α-syn immune complex significantly increased the level of Fcγ receptor on the microglia (Fig. 10B).

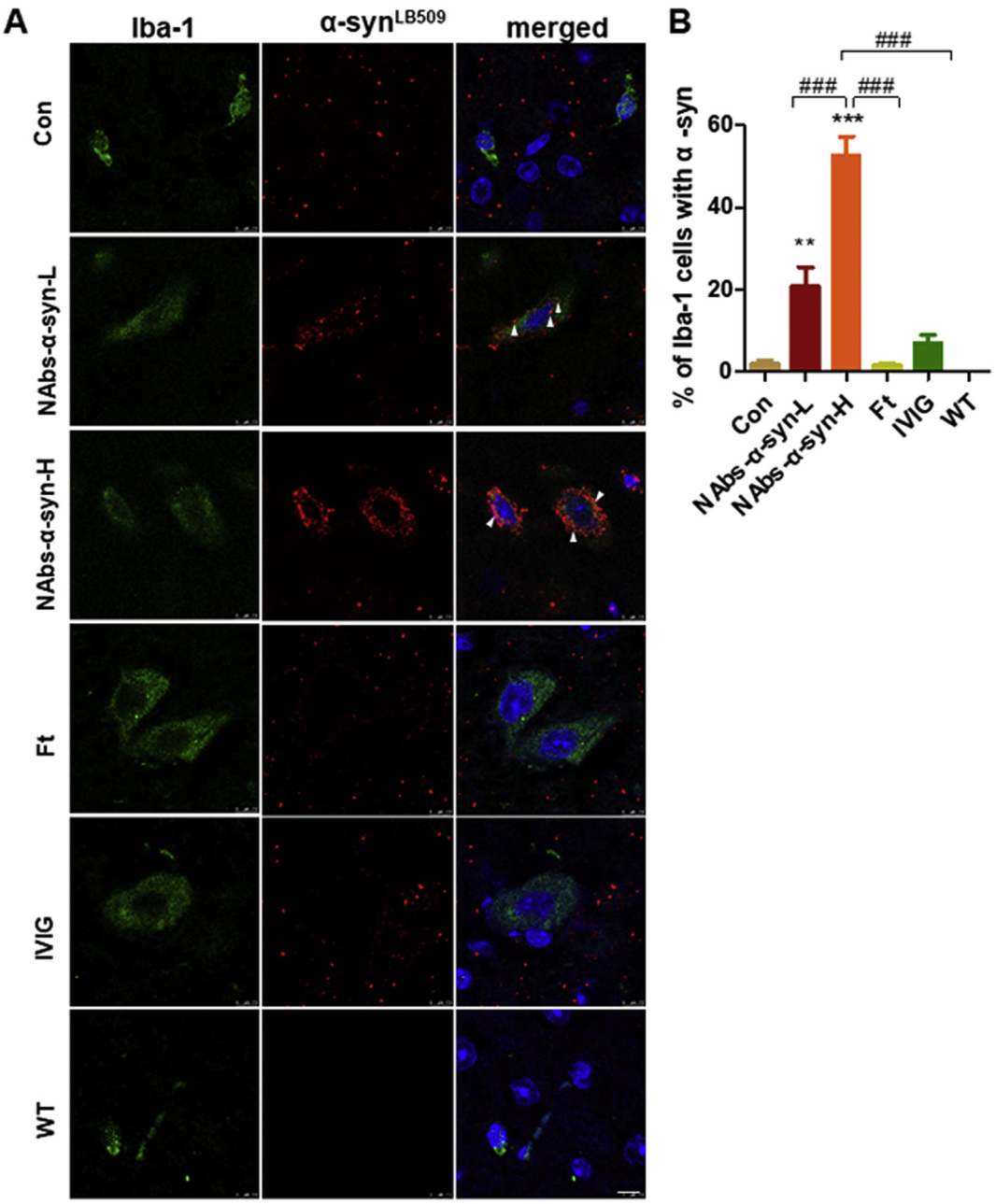

Fig. 9. NAbs-α-syn promoted the uptake of α-syn by microglia. (A) A53T tg mice were treated with vehicle, low dose or high dose of NAbs-α-syn, Ft or IVIG, respectively. The microglia and α-syn deposits in the brain stems were detected by anti-Iba-1 and anti-α-syn antibodies, respectively, then the data were quantified using IpWin5 software (B). Arrowheads indicate colocalization of α-syn and microglia. Scale bar, 10 μm. Statistical analysis: one-way ANOVA followed by Tukey's test (compared with Con, $^{**}P < .01$, $^{***}p < .001$, compared with NAbs-α-syn-H, $^{###}p < .001$).

4. Discussion

IVIG, which contains thousands of monoclonal antibodies against different antigens, is manufactured from pooled plasma of thousands of healthy donors and has been used safely in the treatment of various diseases (Hughes et al., 2009; Lunemann et al., 2015), but the amount of antibodies in IVIG against one antigen or pathogen is extremely low, that is why it often failed to obtain ideal outcome when using IVIG for disease-modified treatment. For example, IVIG failed to improve the cognition and memory in the patients of AD in phase III clinical trials (Relkin, 2014). To overcome this deficiency of IVIG, we here isolated polyclonal NAbs-α-syn from IVIG and investigated their biochemical properties in vitro and behavioral effects in PD transgenic mice.

In the progression of PD, α-syn undergoes conformational changes to become toxic oligomers, which may induce the progressive death of dopamine-producing neurons in the substantia nigra of the midbrain which is located within the brainstem, leading to motor and cognitive deficits (Savitt et al., 2006). Therefore, reducing the level of α-syn in the patient's brains is a major strategy for the treatment of PD. Our NAbs-α-syn contained antibodies against monomers, oligomers, which were much condensed by the affinity chromatography. Therefore, at the same concentration of the antibody protein, NAbs-α-syn inhibited α-syn aggregation and cytotoxicity much more effectively than IVIG in vitro. Consistently, NAbs-α-syn rather than IVIG, Ft significantly reduced the levels of soluble α-syn and OC-positive α-syn oligomers in the brain stems and improved the cognitive and motor deficits of PD mice. Besides, our results also showed that IVIG exerted some beneficial effects by improving motor deficits and attenuating α-syn pathology in A53T

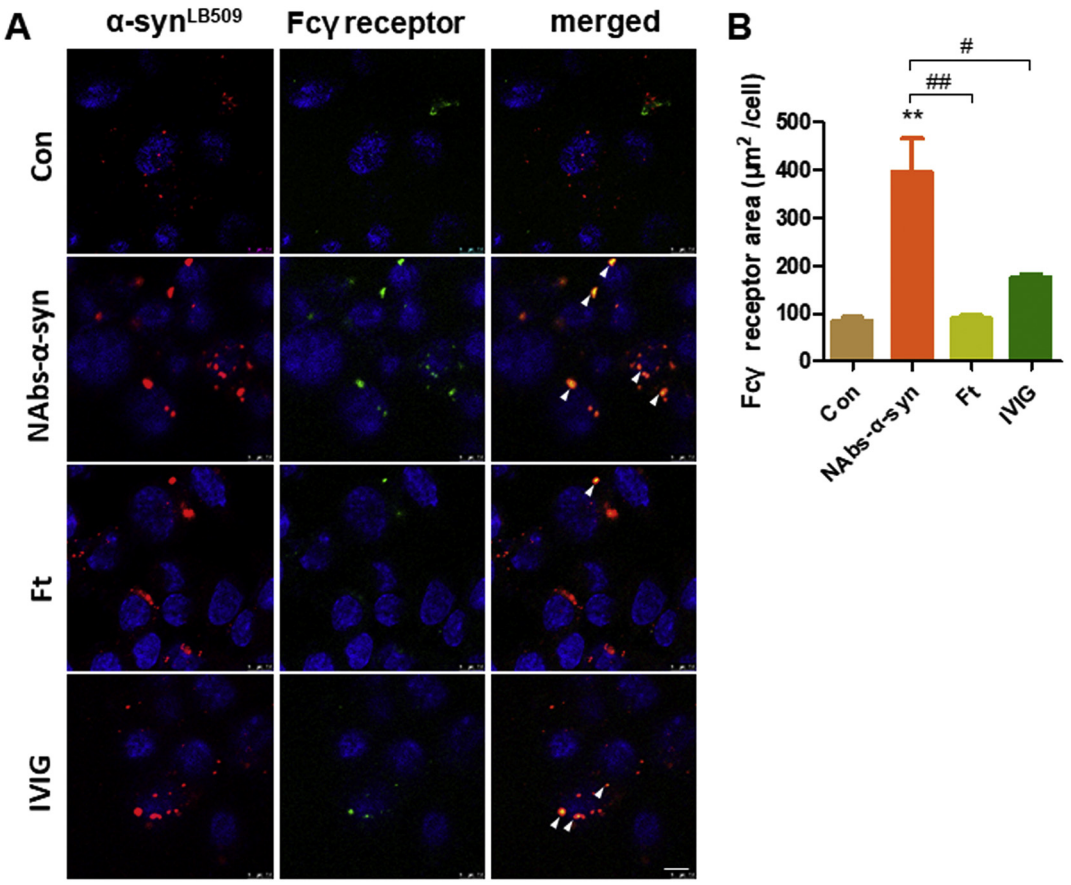

Fig. 10. NAbs-α-syn promoted the expression of Fcγ receptors in vitro. (A) NAbs-α-syn promoted the expression of Fcγ receptor on BV2 cells. Complexes of α-syn with NAbs-α-syn, IVIG or Ft were added to BV2 cells. α-syn (red) and Fcγ receptors (green) on BV2 cells were detected 24 h later. Scale bars, 7.5 μm. (B) The data of Fcγ receptors were quantified using IpWin5 software. Statistical analysis: one-way ANOVA followed by Tukey's test (compared with Con, $^{**}P < .01$, compared with NAbs-α-syn-H, $^{\#}p < .05$, $^{\#\#}p < .01$). (For interpretation of the references to colour in this figure legend, the reader is referred to the web version of this article.)

mice, which was in contrast with the results of Isabelle et al. that IVIG didn't reverse the neuronal damage in MPTP mice (St-Amour et al., 2012). These distinct results may be because of different PD models used for the investigation. A53T mice used in our study overexpressed A53T α-syn to which IVIG might bind, but MPTP mice was constructed by injecting MPTP on which IVIG might have no effect. Moreover, Ft contained antibodies against α-syn monomers and fibrils, and did not show apparent effect on motor deficits and α-syn pathology of A53T mice, indicating that α-syn oligomer-specific antibodies may play a key role in the treatment of PD mice. Our previous report also showed that the naturally occurring autoantibodies against Aβ oligomers (NAbs-Aβo) isolated from IVIG rescued memory deficits and attenuated Aβ pathology in AD transgenic mice (Wang et al., 2016). NAbs-Aβo also exhibited more beneficial effects in the treatment of AD transgenic mice than IVIG.

Omar et al. reported that antibodies Syn-O1 and −O4 against early stage oligomers of α-syn were superior to antibody Syn-O2 against late stage oligomers when treating line 61 α-syn transgenic model (El-Agnaf et al., 2017). Our NAbs-α-syn purified by the α-syn oligomers with lower molecular weight may also target early oligomers, accounting for the benefit on the treatment of PD mice. TH is a rate-limiting enzyme involved in DA generation, its level is inversely correlated with the total α-syn burden in the substantia nigra of PD patients or animal models (Arawaka et al., 2014; Matsuoka et al., 2001; Kovacs et al., 2008). Our results indicated that NAbs-α-syn increased levels of TH in the striatum and brain stems of A53T α-syn mice by decreasing α-syn level, thus protecting neuronal cells from degeneration.

Previous report showed that over-expression of α-syn increased the level of pro-inflammatory MCP-1 (CCL2), which may recruit CCR2 + monocytes from periphery to substantia nigra (Harms et al., 2018). These CCR2 + monocytes induced the pro-inflammatory MHCII response in the SNpc, resulting in degeneration of dopaminergic neurons. Our results showed that treatment with NAbs-α-syn decreased the level of MCP-1, which may partly contribute to prevention of α-syn-induced neuronal degeneration. α-syn aggregates may also induce astrocytosis and microgliosis in the brains of PD patients and corresponding mouse models, which contributes to the progression of PD (Ouchi et al., 2009). Previous reports showed that Iba-1 was highly and specifically expressed in microglia, and its expression was upregulated by inflammation (Ito et al., 1998). GFAP is expressed in astrocytes, and its expression is also significantly increased by inflammation in PD patients (Dauer and Przedborski, 2003). Therefore, we used Iba-1 and GFAP as glia markers to detect microgliosis and astrogliosis. In agreement with previous reports (El-Agnaf et al., 2017), our antibodies against α-syn oligomers significantly suppressed activation of microglia and astrocytes.

To date, the mechanism underlying the antibody-induced cognitive improvement in PD patients or mice remains unknown. Previous reports showed that active immunization with α-syn or passive immunization with antibodies protected against neurodegeneration and reduced α-syn accumulation by promoting α-syn clearance via autophagy, microglia or lysosomal pathways (Bae et al., 2012; Kallab et al., 2018; Sanchez-Guajardo et al., 2013; Masliah et al., 2005). In addition, immunization might also be of therapeutic benefit by decreasing α-syn propagation (Games et al., 2014; Bae et al., 2012; Valera and Masliah, 2013). Consistent with previous reports, our results also showed that NAbs-α-syn attenuated α-syn pathology probably by promoting microglia clearance via Fcγ receptors.

As the volunteers' own immune systems may be constantly exposed to α-syn aggregates and perform affinity maturation, NAbs-α-syn is naturally potent. In contrast to a single monoclonal antibody targeting only an epitope of α-syn aggregates, polyclonal NAbs-α-syn can bind to various pathological α-syn aggregates, which may provide more benefit in treating PD (Hatami et al., 2014). In addition, NAbs-α-syn isolation from IVIG may not interfere with the normal function of conventional IVIG as its concentration is very low. Thus, the isolated NAbs-α-syn as an extra product of plasma requires low cost and is feasible for PD treatment.

In conclusion, our study first demonstrated that the NAbs-α-syn purified from IVIG bound to α-syn monomers and oligomers and exerted favorable effect on cognitive and motor deficits by inhibiting α-syn aggregation and cytotoxicity, decreasing the levels of soluble α-syn, total human α-syn, α-syn oligomers and deposits, reducing axonal pathology, increasing the levels of PSD95, synaptophysin and TH, and suppressing microgliosis, astrogliosis, and proinflammatory cytokine production in the A53T transgenic mouse brains. Our results suggested that NAbs-α-syn may be a safer and effective immunotherapy for the treatment of PD.

Acknowledgements

This work was supported by the grants from the Strategic Leading Project of China Academy of Sciences (XDA 12040215) and the National Science and Technology Major Projects of New Drugs (2015ZX09102015).

References

Arawaka, S., et al., 2014. Zonisamide attenuates alpha-synuclein neurotoxicity by an aggregation-independent mechanism in a rat model of familial Parkinson's disease. PLoS One 9, e89076.
Bae, E.J., et al., 2012. Antibody-aided clearance of extracellular alpha-synuclein prevents cell-to-cell aggregate transmission. J. Neurosci. 32, 13454–13469.
Bellucci, A., Navarria, L., Zaltieri, M., Missale, C., Spano, P., 2012. alpha-Synuclein synaptic pathology and its implications in the development of novel therapeutic approaches to cure Parkinson's disease. Brain Res. 1432, 95–113.
Brundin, P., Melki, R., Kopito, R., 2010. Prion-like transmission of protein aggregates in neurodegenerative diseases. Nat. Rev. Mol. Cell Biol. 11, 301–307.
Dauer, W., Przedborski, S., 2003. Parkinson's disease: mechanisms and models. Neuron 39, 889–909.
Desplats, P., et al., 2009. Inclusion formation and neuronal cell death through neuron-to-neuron transmission of alpha-synuclein (vol 106, pg 13010, 2009). Proc. Natl. Acad. Sci. U. S. A. 106, 13010–13015.
El-Agnaf, O., et al., 2017. Differential effects of immunotherapy with antibodies targeting alpha-synuclein oligomers and fibrils in a transgenic model of synucleinopathy. Neurobiol. Dis. 104, 85–96.
Games, D., et al., 2013. Axonopathy in an alpha-synuclein transgenic model of Lewy body disease is associated with extensive accumulation of C-terminal-truncated alpha-synuclein. Am. J. Pathol. 182, 940–953.
Games, D., et al., 2014. Reducing C-terminal-truncated alpha-synuclein by immunotherapy attenuates neurodegeneration and propagation in Parkinson's disease-like models. J. Neurosci. 34, 9441–9454.
Gaugler, M.N., et al., 2012. Nigrostriatal overabundance of α-synuclein leads to decreased vesicle density and deficits in dopamine release that correlate with reduced motor activity. Acta Neuropathol. 123, 653–669.
Gessner, J.E., Heiken, H., Tamm, A., Schmidt, R.E., 1998. The IgG Fc receptor family. Ann. Hematol. 76, 231–248.
Graham, D.R., Sidhu, A., 2010. Mice expressing the A53T mutant form of human alpha-synuclein exhibit hyperactivity and reduced anxiety-like behavior. J. Neurosci. Res. 88, 1777–1783.
Gustafsson, G., et al., 2017. Alpha-synuclein oligomer-selective antibodies reduce intracellular accumulation and mitochondrial impairment in alpha-synuclein exposed astrocytes. J. Neuroinflammation 14, 241.
Harms, A.S., et al., 2018. Peripheral monocyte entry is required for alpha-Synuclein induced inflammation and Neurodegeneration in a model of Parkinson disease. Exp. Neurol. 300, 179–187.
Hatami, A., Albay 3rd, R., Monjazeb, S., Milton, S., Glabe, C., 2014. Monoclonal antibodies against Abeta42 fibrils distinguish multiple aggregation state polymorphisms in vitro and in Alzheimer disease brain. J. Biol. Chem. 289, 32131–32143.
Hoyer, W., et al., 2002. Dependence of α-synuclein aggregate morphology on solution conditions. J. Mol. Biol. 322, 383–393.
Hughes, R.A., et al., 2009. Clinical applications of intravenous immunoglobulins in neurology. Clin. Exp. Immunol. 158 (Suppl. 1), 34–42.
Hunt, C.A., Schenker, L.J., Kennedy, M.B., 1996. PSD-95 is associated with the postsynaptic density and not with the presynaptic membrane at forebrain synapses. J. Neurosci. 16, 1380–1388.
Ito, D., et al., 1998. Microglia-specific localisation of a novel calcium binding protein, Iba1. Brain Res. Mol. Brain Res. 57, 1–9.
Jakes, R., Spillantini, M.G., Goedert, M., 1994. Identification of two distinct synucleins from human brain. FEBS Lett. 345, 27–32.
Jankovic, J., et al., 2017. Results from a phase 1b multiple ascending-dose study of PRX002, an anti-alpha-synuclein monoclonal antibody, in patients with Parkinson's Disease. Eur. J. Neurol. 24, 211–218.
Kallab, M., et al., 2018. Region-specific effects of immunotherapy with antibodies targeting alpha-synuclein in a transgenic model of synucleinopathy. Front. Neurosci. 12, 452.
Kayed, R., et al., 2007. Fibril specific, conformation dependent antibodies recognize a generic epitope common to amyloid fibrils and fibrillar oligomers that is absent in prefibrillar oligomers. Mol. Neurodegener. 2, 18.
Kim, J.Y., Jeon, B.S., Kim, H.J., Ahn, T.B., 2013. Nanomolar concentration of alpha-synuclein enhances dopaminergic neuronal survival via Akt pathway. Neural Regen. Res. 8, 3269–3274.
Kovacs, G.G., Milenkovic, I.J., Preusser, M., Budka, H., 2008. Nigral burden of alpha-synuclein correlates with striatal dopamine deficit. Mov. Disord. 23, 1608–1612.
Lee, H.J., Lee, S.J., 2002. Characterization of cytoplasmic alpha-synuclein aggregates - Fibril formation is tightly linked to the inclusion-forming process in cells. J. Biol. Chem. 277, 48976–48983.
Lee, M.K., et al., 2002. Human alpha-synuclein-harboring familial Parkinson's disease-linked Ala-53 – > Thr mutation causes neurodegenerative disease with alpha-synuclein aggregation in transgenic mice. Proc. Natl. Acad. Sci. U. S. A. 99, 8968–8973.
Lee, H.J., et al., 2010. Direct transfer of alpha-synuclein from neuron to astroglia causes inflammatory responses in synucleinopathies. J. Biol. Chem. 285, 9262–9272.
Liu, P., et al., 2015. Quaternary structure defines a large class of amyloid-beta oligomers neutralized by sequestration. Cell Rep. 11, 1760–1771.
Lunemann, J.D., Nimmerjahn, F., Dalakas, M.C., 2015. Intravenous immunoglobulin in neurology-mode of action and clinical efficacy. Nat. Rev. Neurol. 11, 80–89.
Masliah, E., et al., 2005. Effects of alpha-synuclein immunization in a mouse model of Parkinson's disease. Neuron 46, 857–868.
Matsuoka, Y., et al., 2001. Lack of nigral pathology in transgenic mice expressing human alpha-synuclein driven by the tyrosine hydroxylase promoter. Neurobiol. Dis. 8, 535–539.
McKeith, I.G., Burn, D., 2000. Spectrum of Parkinson's disease, Parkinson's dementia, and lewy body dementia. Neurol. Clin. 18, 865.
Meredith, G.E., Kang, U.J., 2006. Behavioral models of Parkinson's disease in rodents: a new look at an old problem. Mov. Disord. 21, 1595–1606.
Metz, G.A., Schwab, M.E., 2004. Behavioral characterization in a comprehensive mouse test battery reveals motor and sensory impairments in growth-associated protein-43 null mutant mice. Neuroscience 129, 563–574.
Migaud, M., et al., 1998. Enhanced long-term potentiation and impaired learning in mice with mutant postsynaptic density-95 protein. Nature 396, 433–439.
Murphy, D.D., Rueter, S.M., Trojanowski, J.Q., Lee, V.M., 2000. Synucleins are developmentally expressed, and alpha-synuclein regulates the size of the presynaptic vesicular pool in primary hippocampal neurons. J. Neurosci. 20, 3214–3220.
Ouchi, Y., Yagi, S., Yokokura, M., Sakamoto, M., 2009. Neuroinflammation in the living brain of Parkinson's disease. Parkinsonism Relat. Disord. 15 (Suppl. 3), S200–S204.
Overk, C.R., Masliah, E., 2014. Pathogenesis of synaptic degeneration in Alzheimer's disease and Lewy body disease. Biochem. Pharmacol. 88, 508–516.
Patrias, L.M., Klaver, A.C., Coffey, M.P., Loeffler, D.A., 2011. Specific antibodies to soluble alpha-synuclein conformations in intravenous immunoglobulin preparations (vol 161, pg 527, 2010). Clinical and Experimental Immunology 166, 527–535.
Pieri, L., Madiona, K., Melki, R., 2016. Structural and functional properties of prefibrillar alpha-synuclein oligomers. Sci. Rep. 6, 24526.
Plotegher, N., et al., 2017. DOPAL derived alpha-synuclein oligomers impair synaptic vesicles physiological function. Sci. Rep. 7, 40699.
Relkin, N., 2014. Clinical trials of intravenous immunoglobulin for Alzheimer's disease. J. Clin. Immunol. 34 (Suppl. 1), S74–S79.
Robinson, S.R., Bishop, G.M., Lee, H.G., Munch, G., 2004. Lessons from the AN 1792 Alzheimer vaccine: lest we forget. Neurobiol. Aging 25, 609–615.
Rostami, J., et al., 2017. Human astrocytes transfer aggregated alpha-synuclein via tunneling nanotubes. J. Neurosci. 37, 11835–11853.
Roy, S., Winton, M.J., Black, M.M., Trojanowski, J.Q., Lee, V.M., 2007. Rapid and intermittent cotransport of slow component-b proteins. J. Neurosci. 27, 3131–3138.
Sanchez-Guajardo, V., Annibali, A., Jensen, P.H., Romero-Ramos, M., 2013. alpha-Synuclein vaccination prevents the accumulation of parkinson disease-like pathologic inclusions in striatum in association with regulatory T cell recruitment in a rat model. J. Neuropathol. Exp. Neurol. 72, 624–645.
Savica, R., Grossardt, B.R., Bower, J.H., Ahlskog, J.E., Rocca, W.A., 2013. Incidence and pathology of synucleinopathies and tauopathies related to parkinsonism. JAMA Neurol. 70, 859–866.
Savitt, J.M., Dawson, V.L., Dawson, T.M., 2006. Diagnosis and treatment of Parkinson disease: molecules to medicine. J. Clin. Invest. 116, 1744–1754.
Scott, D.A., et al., 2010. A pathologic cascade leading to synaptic dysfunction in α-synuclein-induced neurodegeneration. J. Neurosci. 30, 8083–8095.
Smith, L.M., Klaver, A.C., Coffey, M.P., Dang, L., Loeffler, D.A., 2012. Effects of intravenous immunoglobulin on alpha synuclein aggregation and neurotoxicity. Int. Immunopharmacol. 14, 550–557.
St-Amour, I., et al., 2012. Impact of intravenous immunoglobulin on the dopaminergic system and immune response in the acute MPTP mouse model of Parkinson's disease. J. Neuroinflammation 9, 234.
Tarnow, I., Nymark, K., Vinge, M., Nielsen, K.A., Ganslandt, C., A Randomized, Double-

Blind, Placebo-Controlled, Single-Centre, 2016. Single ascending dose and multiple ascending dose study of the safety, tolerability, pharmacokinetics, and pharmacodynamics of molgramostim (rhgm-Csf) administered by inhalation to healthy adult subjects. American Journal of Respiratory and Critical Care Medicine 193.

Trojanowski, J.Q., Lee, V.M.Y., 1998. Aggregation of neurofilament and alpha-synuclein proteins in Lewy bodies - Implications for the pathogenesis of Parkinson disease and Lewy body dementia. Arch. Neurol. 55, 151–152.

Tsigelny, I.F., et al., 2007. Dynamics of alpha-synuclein aggregation and inhibition of pore-like oligomer development by beta-synuclein. FEBS J. 274, 1862–1877.

Valera, E., Masliah, E., 2013. Immunotherapy for neurodegenerative diseases: focus on alpha-synucleinopathies. Pharmacol. Ther. 138, 311–322.

Wang, T., et al., 2016. Naturally occurring autoantibodies against A beta oligomers exhibited more beneficial effects in the treatment of mouse model of Alzheimer's disease than intravenous immunoglobulin. Neuropharmacology 105, 561–576.

Wang, S.W., et al., 2017. A vaccine with Abeta oligomer-specific mimotope attenuates cognitive deficits and brain pathologies in transgenic mice with Alzheimer's disease. Alzheimers Res. Ther. 9, 41.

Weihofen, A., et al., 2016. Human-derived alpha-synuclein antibody BIIB054 binds pathologic forms of alpha-synuclein and attenuates transmission of alpha-synuclein in vitro and in vivo (abstract). Mov. Disord. 31 (suppl 2).